

Faculty of Engineering
Faculty of Engineering - Papers

University of Wollongong

Year 2006

Room-temperature ferromagnetism in
Mn and Fe codoped In₂O₃

G. Peleckis* X. L. Wang[†]
S. X. Dou[‡]

*University of Wollongong

[†]University of Wollongong, xiaolin@uow.edu.au

[‡]University of Wollongong, shi@uow.edu.au

This article was originally published as: Peleckis, G, Wang, XL & Dou, SX, Room-temperature ferromagnetism in Mn and Fe codoped In₂O₃, Applied Physics Letters, 2006, 88, 132507. Original journal available here.

This paper is posted at Research Online.

<http://ro.uow.edu.au/engpapers/133>

Room-temperature ferromagnetism in Mn and Fe codoped In_2O_3

G. Peleckis, X. L. Wang,^{a)} and S. X. Dou

Institute for Superconducting and Electronic Materials, University of Wollongong, Wollongong, New South Wales 2522, Australia

(Received 2 June 2005; accepted 7 March 2006; published online 28 March 2006)

The synthesis and characterization of polycrystalline room-temperature ferromagnetic semiconductor $(\text{In}_{0.9}\text{Fe}_{0.1-x}\text{Mn}_x)_2\text{O}_3$ ($x=0-0.1$) oxide are reported. All of the samples with intermediate x values are ferromagnetic at room temperature. The highest saturation magnetization moment at 300 K per total amount of magnetic ion is reached in the $(\text{In}_{0.9}\text{Fe}_{0.04}\text{Mn}_{0.06})_2\text{O}_3$ sample. The lattice constant a increases linearly with increasing Mn content. Fe-only doped samples were paramagnetic, while a Mn-only doped sample was found to be ferromagnetic below $T_C=46$ K. © 2006 American Institute of Physics. [DOI: 10.1063/1.2191093]

After reported ferromagnetism in Mn-doped GaAs,¹ considerable research was concentrated on finding new semiconductors that can exhibit ferromagnetic feature. Usually diluted magnetic semiconductors (DMSs) are formed when transition metal ions, such as 3d elements, are doped into the host lattice of a semiconductor. Many materials have been found, which could be considered as good candidates for DMS applications.²⁻⁶ However, due to the small solubility of magnetic ions in the host semiconductor, ferromagnetism in some cases is attributed to the clusters of dopants formed during the sample preparation procedure.⁷⁻⁹ Therefore, new diluted magnetic semiconductors based on host semiconductors with high solubility of transition metal ions are highly desirable.

Recently Yoo *et al.*¹⁰ and He *et al.*¹¹ have reported both polycrystalline bulks and thin film samples of a diluted magnetic semiconductor—Fe and Cu codoped In_2O_3 oxides. The solubility of Fe ions in the host compound was found to be around 20%. In order to achieve multivalence and thus ferromagnetism, some Cu was codoped along with Fe.^{10,11} Their samples show clear ferromagnetic features at room temperature. In addition, both articles investigated the possible contribution of magnetic impurities to the ferromagnetism in detail, showing that the ferromagnetism in their samples is intrinsic. Mn is a very good agent to introduce multivalent species in addition to its high magnetic moment. Thus, we expected that when codoped with Fe it would enhance ferromagnetism in In_2O_3 . In this Letter we report on the observation of room-temperature ferromagnetism in Fe–Mn codoped In_2O_3 polycrystalline samples.

$(\text{In}_{0.9}\text{Fe}_{0.1-x}\text{Mn}_x)_2\text{O}_3$ ($0 \leq x \leq 0.1$) polycrystalline samples were prepared by a conventional solid state synthesis technique. Starting materials of In_2O_3 , Fe_2O_3 , and MnCO_3 (with all material high purity: 99.99%; Aldrich) were weighed and mixed in a mortar in corresponding ratios to obtain nominal chemical compositions for the final products. Mixed powders were calcined in an argon atmosphere at 850 °C for 12 h. After that, the reacted material was ground in a mortar, pressed into rectangular shaped pellets, and fired at 950 °C for 12 h in an argon atmosphere with further annealing at 970 °C in an argon atmosphere for various periods (10–48 h). The phases and crystal structure of

samples were analyzed by means of x-ray diffraction technique using Cu $K\alpha$ irradiation (Mac Science; M03 XHF22). X-ray diffraction patterns were refined applying Rietveld refinement technique using RIETICA software.¹² The x-ray diffraction patterns for all the samples can be indexed based on the unit cell of a cubic In_2O_3 .¹³ The observed, calculated, and difference diffraction profiles for all the samples are shown in Fig. 1. It can be seen that the refinement results are in excellent agreement with the experimental data. Two end compounds with $x=0$ and 0.1, i.e., $(\text{In}_{0.9}\text{Fe}_{0.1})_2\text{O}_3$ and $(\text{In}_{0.9}\text{Mn}_{0.1})_2\text{O}_3$, and $x=0.02$ and 0.08 obviously are of single phase, as no any other visible peaks present in these samples, as shown in the inset of Fig. 1. Close examinations of diffraction profiles revealed presence of tiny traces of MnFe_2O_4 as a secondary phase in samples with $x=0.04$ and 0.06. The amounts of this impurity have been determined to be 0.34 and 0.13 wt % for $x=0.04$ and 0.06, respectively, after numerous high quality Rietveld refinements with goodness factors $R_p=10.98$, $R_{wp}=14.75$, and $\chi^2=0.97$ ($x=0.04$) and $R_p=9.72$, $R_{wp}=14.43$, and $\chi^2=0.91$ ($x=0.06$). The dependence of the lattice parameter a (obtained by refinement analyses) on x is represented in the left inset of Fig. 1. With increasing

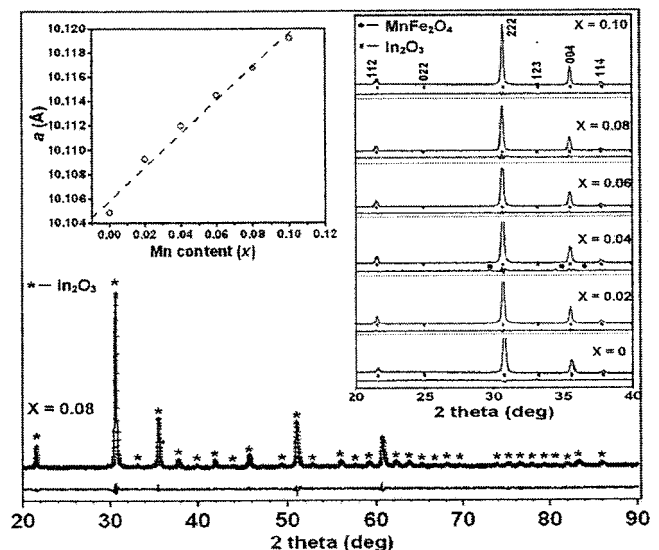


FIG. 1. Rietveld refinement of x-ray diffraction pattern for sample with $x=0.08$. Insets: right—magnified view of Rietveld refinements for samples with different x ; left—dependence of lattice parameter a on Mn content x .

^{a)}Electronic mail: xiaolin@uow.edu.au

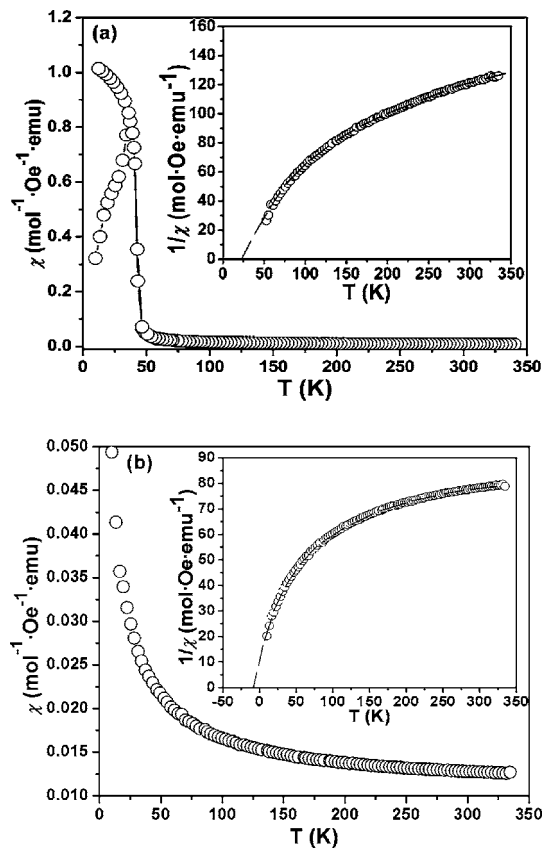


FIG. 2. Magnetic susceptibility (χ) vs temperature (T): (a) $(\text{In}_{0.9}\text{Mn}_{0.1})_2\text{O}_3$ and (b) $(\text{In}_{0.9}\text{Fe}_{0.1})_2\text{O}_3$ samples under 2000 Oe applied magnetic field. Insets represent the inverse magnetic susceptibility ($1/\chi$) data under the same conditions with modified Curie-Weiss law fittings.

Mn content the lattice parameter a increased almost linearly, from $a=10.109$ Å to $a=10.118$ Å, when x rose from 0 to 0.1, respectively. The obtained dependence of lattice parameter a on Mn content is in a good agreement with data published by Yoo *et al.*,¹⁰ where they showed a decrease in a with increasing Fe content. This result is reasonable if the ionic radii of Mn and Fe are compared. If we assume that both magnetic ions, i.e., Mn and Fe, are present in oxidation state of 3+ in octahedral configuration, then $r_{i(\text{Mn}^{2+})}=0.72$ Å and $r_{i(\text{Fe}^{3+})}=0.69$ Å.¹⁴ This indicates that the expansion of the lattice parameter a is due to the bigger ionic size of Mn^{3+} ions. The change in lattice parameter a suggests that magnetic ions were successfully introduced into the crystal structure of In_2O_3 .

The molar magnetic susceptibility (χ) versus temperature (T) curves for $(\text{In}_{0.9}\text{Mn}_{0.1})_2\text{O}_3$ and $(\text{In}_{0.9}\text{Fe}_{0.1})_2\text{O}_3$ samples is shown in Figs. 2(a) and 2(b), respectively. The zero field cooled (ZFC) measurements were done during warming in a field of 2000 Oe (Quantum Design, MPMS XL). The insets of Figs. 2(a) and 2(b) depict the inverse magnetic susceptibility ($1/\chi$) as a function of T . There are distinct differences in the magnetic properties for these samples. The Fe-only doped sample showed paramagnetic behavior over the whole temperature range, while the Mn-only doped sample exhibits ferromagnetic features below $T_C=46$ K. The observed paramagnetism for the Fe-only doped sample contradicts the observed ferromagnetism in Fe-doped In_2O_3 as reported in Ref. 10, which is probably caused by lack of multivalent magnetic ions in the material.

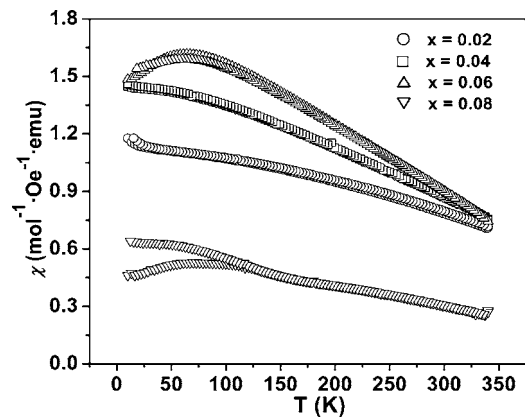


FIG. 3. Magnetic susceptibility (χ) as a function of temperature (T) for samples with $0 < x < 1$ under 2000 Oe applied magnetic field.

The data for inversed susceptibility curves ($1/\chi$) [insets of Figs. 2(a) and 2(b)] were fitted by applying the modified Curie-Weiss law:

$$\chi = \frac{C}{T - \Theta_p} + \chi_0, \quad (1)$$

where χ_0 is the temperature independent susceptibility (sum of Pauli, Landau, and core susceptibilities), and Θ_p is the Pauli-Weiss temperature. The calculated Θ_p values were -8.13 and 23.97 K for $x=0$ and 0.1, respectively. The calculated effective magnetic moments (μ_{eff}) from Eq. (1) are $\mu_{\text{eff}}=2.87\mu_B/\text{Mn}$ and $\mu_{\text{eff}}=2.25\mu_B/\text{Fe}$ for Mn- and Fe-doped samples, respectively. The spin state assessment for the sample with $x=0$ showed that Fe is present as Fe^{3+} in a low spin (LS) state. On the other hand the calculated $\mu_{\text{eff}}=2.87\mu_B/\text{Mn}$ for sample with $x=0.1$ corresponds to that of Mn^{3+} in an intermediate spin (IS) state.

Figure 3 represents the dependence of molar magnetic susceptibility (χ) on temperature (T) for samples with intermediate x values ($0 < x < 0.1$). The measurement conditions were the same as for Mn- and Fe-only doped samples. It can be seen that all the samples are ferromagnetic at room temperature. One could argue that the observed room-temperature ferromagnetism arises from the impurity phase (MnFe_2O_4).^{15,16} However, if the observed magnetization is contributed only from the MnFe_2O_4 phase, then the calculated magnetization should be close to 40 emu/g at 5 K and $H > 3$ T.^{15,16} In fact, we have prepared pure impurity sample of MnFe_2O_4 using the same preparation conditions for all other samples used in this work. Our MnFe_2O_4 samples showed a magnetization of 43 emu/g at 10 K and $H > 3$ T, the same as that reported for MnFe_2O_4 . Sample with $x=0.06$ gives a magnetization of ~ 400 emu/g at 10 K in a field $H > 2$ T, if only MnFe_2O_4 contribution is considered. This value is one order of magnitude greater than that reported for pure MnFe_2O_4 ,^{15,16} implying that the tiny amount of MnFe_2O_4 impurity make little contribution to the magnetization observed in our codoped In_2O_3 samples with $x=0.04$ and 0.06. In addition, if the contribution from MnFe_2O_4 phase is deducted from χ - T curves, calculated difference between curves is less than 1%. Furthermore, if the observed ferromagnetic feature arises only from the impurity phase, the values of magnetization should be proportional to the amount of impurity present in the system, i.e., sample with $x=0.04$ should have highest values of magnetization

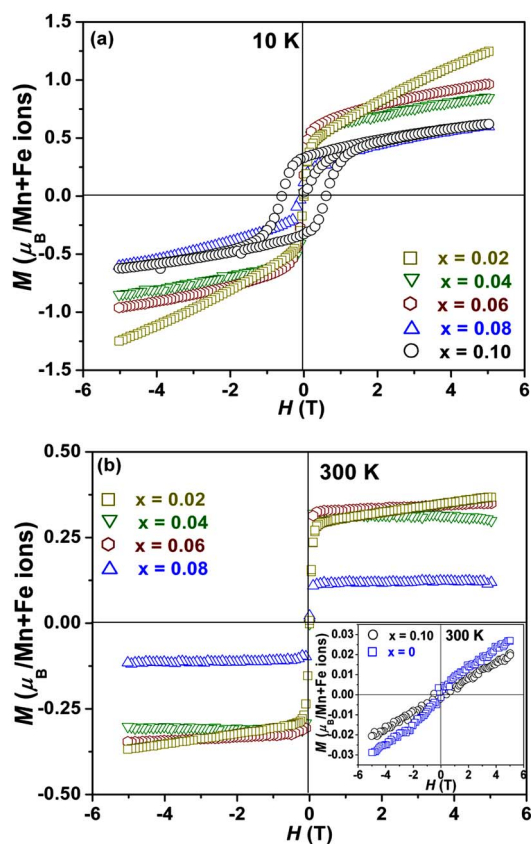


FIG. 4. (Color online) Dependence of magnetization (M) per total magnetic ion (Mn+Fe) on applied magnetic field (H): $(\text{In}_{0.9}\text{Fe}_{1-x}\text{Mn}_x)_2\text{O}_3$ samples at constant temperatures of (a) 10 K and (b) 300 K. M is expressed in $\mu_B/(\text{Mn}+\text{Fe})$. Inset shows M - H curves for samples with $x=0$ and 0.1 at 300 K.

which is not the case in our samples. Another strong fact is that there are significant differences in irreversibility of the χ - T curves for different Mn content x (Fig. 3). Lastly, magneto-optical imaging (MOI) revealed that samples with intermediate x values magnetized homogeneously and showed no sign of localized domains formed by MnFe_2O_4 impurity. These findings strongly suggested that observed ferromagnetism is rather an intrinsic property of the material.

Figure 4(a) shows magnetization (M) versus applied magnetic field (H) at 10 K for all the samples. As the x value increases there is a distinct ferromagnetic response in the M - H curves. The maximal value of magnetization of $0.98\mu_B/(\text{Mn}+\text{Fe})$ ion was achieved for $x=0.06$. The Mn-only doped sample shows a high coercive field H_c of about 5000 Oe. Magnetization data of the samples at 300 K are given in Fig. 4(b). Here both end compounds, i.e., $x=0$ and $x=0.1$, show no trace of ferromagnetism [inset of Fig. 4(b)]. It can be seen that magnetizations at 300 K saturate at a small field of 0.1 T for samples with $x=0.04$, 0.06, and 0.08. The saturation magnetization (M_s) of these samples increased and reached a maximal value of $M_s=0.35\mu_B/(\text{Mn}+\text{Fe})$ when $x=0.06$, and then dropped, when $x>0.06$. Yoo *et*

*al.*¹⁰ found that Fe^{3+} in a high spin (HS) state contributed to the saturation magnetization in Fe-doped In_2O_3 . In contrast to their result, we found that for both samples with $x=0.06$ and 0.04, the M_s data most likely correspond to that of Fe^{3+} (LS) and Mn^{3+} (IS) states. These values of both valences and spin states support the fact that the lattice expansion was caused by increase/decrease of $\text{Mn}^{3+}/\text{Fe}^{3+}$ content in the samples.

In summary, a series of polycrystalline Fe and Mn codoped $(\text{In}_{0.9}\text{Fe}_{0.1-x}\text{Mn}_x)_2\text{O}_3$ oxide samples was prepared by a conventional solid state synthesis technique. The lattice parameter a increases with increasing Mn content (x). In contrast to the already reported data,¹⁰ the Fe-only ($x=0$) doped sample was paramagnetic at room temperature. The Mn-only ($x=0.1$) doped sample was ferromagnetic below $T_C=46$ K. Samples with $0<x<0.1$ values were ferromagnetic at room temperature. Maximum M_s values of $0.35\mu_B/(\text{Fe}+\text{Mn})$ and $0.98\mu_B/(\text{Fe}+\text{Mn})$ were achieved for $x=0.06$ at 300 and 10 K, respectively, which was in good agreement with the literature data.¹⁰ Further structural and transport studies are essential in order to clarify the nature of observed high temperature ferromagnetism in this material.

This work was supported by the Australian Research Council under Discovery Project DP0558753 to one of the authors (X.L.W.). Another author (G.P.) thanks the Australian government and the University of Wollongong for providing IPRS and UPA scholarships for his Ph.D. studies.

¹H. Ohno, *Science* **281**, 951 (1998).

²K. Ueda, H. Tabata, and T. Kawai, *Appl. Phys. Lett.* **79**, 988 (2001).

³Y. Matsumoto, M. Murakami, T. Shono, H. Hasegawa, T. Fukumura, M. Kawasaki, P. Ahmet, T. Chikyow, S. Koshikara, and H. Koinuma, *Science* **291**, 854 (2001).

⁴D. P. Norto, S. J. Pearton, A. F. Hebard, N. Theodoropoulou, L. A. Boatner, and R. G. Wilson, *Appl. Phys. Lett.* **82**, 239 (2003).

⁵F. Tsui, L. He, L. Ma, A. Tkachuk, Y. S. Chu, K. Nakajima, and T. Chikyow, *Phys. Rev. Lett.* **91**, 177203 (2003).

⁶Z. J. Wang, W. D. Wang, J. K. Tang, L. D. Tung, L. Spinu, and W. Zhou, *Appl. Phys. Lett.* **83**, 518 (2003).

⁷J. H. Kim, H. Kim, D. Kim, Y. E. Ihm, and W. K. Choo, *J. Eur. Ceram. Soc.* **24**, 1847 (2004).

⁸J. H. Park, M. G. Kim, H. M. Jang, S. Ryu, and Y. M. Kim, *Appl. Phys. Lett.* **84**, 1338 (2004).

⁹J. Y. Kim, J. H. Park, B. G. Park, H. J. Noh, S. J. Oh, J. S. Yang, D. H. Kim, S. D. Bu, T. W. Noh, H. J. Lin, H. H. Hsieh, and C. T. Chen, *Phys. Rev. Lett.* **90**, 017401 (2003).

¹⁰Y. K. Yoo, Q. Xue, H.-C. Lee, S. Cheng, X.-D. Xiang, G. F. Dionne, S. Xu, J. He, Y. S. Chu, S. D. Preite, S. E. Lofland, and I. Takeuchi, *Appl. Phys. Lett.* **86**, 042506 (2005).

¹¹J. He, S. Xu, Y. K. Yoo, Q. Xue, H.-C. Lee, S. Cheng, X.-D. Xiang, G. F. Dionne, and I. Takeuchi, *Appl. Phys. Lett.* **86**, 052503 (2005).

¹²B. A. Hunter, *IUCC Powder Diffraction* **20**, 21 (1998).

¹³N. Nadaud, N. Lequeux, M. Nanot, J. Jove, and T. Roisnel, *J. Solid State Chem.* **135**, 140 (1998).

¹⁴R. D. Shannon, *Acta Crystallogr., Sect. A: Cryst. Phys., Diffir., Theor. Gen. Crystallogr.* **32**, 751 (1976).

¹⁵J. Hu, H. Qin, Y. Wang, S. Zhang, and Z. Wang, *J. Mater. Sci. Lett.* **20**, 1531 (2001).

¹⁶J. Wang, C. Zeng, Z. Peng, and Q. Chen, *Physica B* **349**, 124 (2004).